Research Square

Preprints are preliminary reports that have not undergone peer review.
They should not be considered conclusive, used to inform clinical practice,
or referenced by the media as validated information.

The Investigation of Morphological and Thermal Properties of SAN/PMMA/MWCNT Nanocomposites

Afşar Çelik

afsarcelik1971@gmail.com

Van Yuzuncu Yil Universitesi Fen Bilimleri Enstitusu https://orcid.org/0000-0002-5824-8338

Gülşen Tozsin

Research Article

Keywords: SAN/PMMA blends MWCNTs, interfacial localization, phase morphology thermal degradation

Posted Date: June 12th, 2026

DOI: https://doi.org/10.21203/rs.3.rs-9888268/v1

License: This work is licensed under a Creative Commons Attribution 4.0 International License.
Read Full License

The Investigation of Morphological and Thermal Properties of SAN/PMMA/MWCNT Nanocomposites

Afsar Celik*, Gülşen Tozsin
*Institute of Science, Van Yüzüncü Yıl University, 65300, Van, Türkiye
Corresponding author email: afsarcelik1971@gmail.com
ORCID: 0000-0002-5824-8338
Department of Metallurgical and Materials Engineering, Ataturk University, 25240, Erzurum, Türkiye
gulsentozsin@gmail.com
ORCID: 0000-0001-5653-9919

ABSTRACT: This study investigated the effects of multi-walled carbon nanotubes (MWCNTs) on the phase morphology and thermal behavior of poly(styrene-co-acrylonitrile) (SAN)/poly (methyl methacrylate) (PMMA) blend systems, with particular emphasis on the localization behavior of MWCNTs within the phases and at the phase interface. Nanocomposite films with varying SAN/PMMA ratios and MWCNT loadings were prepared via solvent casting and characterized using SEM, FTIR, XRD, DSC, and TGA analyses within a multiscale framework. SEM observations revealed that MWCNTs were preferentially localized at the SAN/PMMA phase interface, where they suppressed phase coalescence and refined the characteristic phase morphology. Although wetting coefficient calculations predicted thermodynamic preference toward the PMMA phase, the experimental findings indicated that solvent evaporation-induced viscosity increase kinetically restricted nanotube migration, leading to interfacial trapping. FTIR analyses showed no evidence of new covalent bond formation, while slight reductions in PMMA carbonyl band intensity suggested steric shielding and reduced functional-group accessibility. XRD results confirmed that the nanocomposites retained their dominant amorphous structure despite MWCNT incorporation. DSC analyses demonstrated a single glass transition temperature (Tg) for all compositions, indicating that the segmental homogeneity and miscibility character of the system were preserved. Thermogravimetric analyses revealed that increasing MWCNT content systematically improved thermal stability, shifted degradation temperatures to higher values, and increased char formation. This behavior was attributed to the discontinuous interfacial MWCNT network, which generated a barrier/labyrinth effect limiting volatile diffusion during degradation. Overall, the results demonstrate that interfacial localized MWCNTs act not only as reinforcing nanofillers but also as morphological regulators governing phase stability and thermal degradation behavior in SAN/PMMA nanocomposite systems.

KEYWORDS: *SAN/PMMA blends MWCNTs, interfacial localization, phase morphology thermal degradation*.

1. INTRODUCTION

Polymer blends are multiphase materials obtained by physically blending two or more polymers without any chemical reactions, which aim to combine the properties of blending polymers and thus optimize the performance. The polymer blend segment is growing approximately three times faster than the broader plastics sector. This trend is driven by both cost optimization and the necessity to achieve the required property combinations.[1] These systems constitute a significant field of research from both academic and industrial perspectives, as they enable targeted combinations of mechanical, optical, and thermal properties to be obtained cost-effectively. It has been reported that global plastic production rose to over 390 million tons in 2023, and demand for engineering plastics continues to grow, particularly in automotive, electronics, and optical applications.[2] However, because most polymer pairs are not thermodynamically miscible, most polymer blends exhibit phase-separated morphologies to varying degrees and in various forms.[3] This morphological structure is a fundamental factor that directly determines the material's final properties.

Polymethyl methacrylate (PMMA) is a transparent thermoplastic notable for its amorphous structure, high light transmittance of approximately 92%, strong weather resistance, and dimensional stability. It is widely used in optical lenses, automotive lighting components, electronic screens, and medical devices.[4] Styrene–acrylonitrile (SAN) copolymer, on the other hand, is an amorphous thermoplastic that provides high hardness, chemical resistance, and surface brightness, and offers a wide range of applications, including housewares, automotive interior parts, and electronic enclosures.[5]

SAN/PMMA blends may offer a balanced property profile between transparency and mechanical and chemical resistance, as they have similar glass transition temperatures and exhibit partial miscibility over specific composition ranges. Therefore, the blends in question attract attention in areas such as surface protection coatings and transparent engineering components, including optical applications, cabin windows, and tail lights.[6] However, the performance of these systems is primarily determined by phase morphology and phase interactions.

Polymeric nanocomposites are materials obtained by dispersing nanometer-sized fillers within a polymer matrix, which can provide distinct mechanical, thermal, and functional

improvements even in low filler contents.[7,8] Within this context, carbon nanotubes (CNTs) are among the most commonly studied nanofillers in polymer-based nanocomposites due to their high aspect ratios and superior electrical and thermal conductivity.[9,10] Electrical conductivity can be achieved at low percolation thresholds, and mechanical and electromagnetic shielding can be improved by adding CNT.[11]

In CNT-reinforced polymer blend systems, one of the principal factors determining the final performance of the material is the distribution of CNTs within the matrix and the localization behavior. The localization of CNTs within a single phase, at a phase interface, or in both phases is determined by thermodynamic and kinetic factors, such as the surface energies of the components, wetting behavior, and process conditions.[12] Particularly in immiscible or partially miscible polymer blends, the localization of CNTs at the phase interface creates a barrier that hinders coalescence/phase merging, thereby stabilizing the phase morphology.

The literature reports that the selective localization behavior of CNTs significantly affects the phase morphology and, consequently, the thermal, mechanical, and functional properties of the material in blend systems containing SAN and PMMA.[12,13] Furthermore, the functionalization of CNT surfaces with functional groups can enhance interactions at the polymer-filler interface, thereby improving charge transfer and thermal performance.[14]

In one of the most comprehensive studies on PMMA/SAN/MWCNT systems, Parameswaranpillai et al.[15] investigated the miscibility, UV resistance, and thermal degradation behavior of PMMA/SAN blends. They showed that adding SAN increased the UV and thermal stability of PMMA, and that low amounts of MWCNT further enhanced this effect. However, their study did not discuss in detail the localization behavior of CNTs within the phase or at the phase interface, nor their role in the evolution of phase morphology.

The present study systematically explored the morphological and thermal properties of nanocomposite films prepared by adding carboxylated multi-walled carbon nanotubes to a SAN/PMMA blend. The primary purpose of this study is to reveal the localization behavior of MWCNTs in the phase morphology and to assess the impacts of this localization on microstructure/morphology and thermal performance from a holistic perspective.

2. MATERIALS AND METHODS

The study used PMMA with an average molecular weight of 350,000, SAN containing 25%, multi-walled carbon nanotubes functionalized with a purity of ≥99% (COOH), and THF (tetrahydrofuran) with a purity of >99%. SAN, PMMA, MWCNT, and THF were obtained from Sigma-Aldrich. The preparation of the nanocomposite followed Celik.[16] SAN/PMMA blends

at 40:60, 50:50, and 60:40 ratios with a total weight of 1 g were prepared by casting from a common solvent. Polymer solutions were prepared at room temperature in a magnetic stirrer at 500 rpm. MWCNTs dispersed in THF at 28–30 °C in an ultrasonic bath were incorporated into the polymer solutions at loadings of 1, 2, 3, and 5 wt%, calculated relative to the polymer blend mass (1 g). This new mixture was stirred for another 2 hours at 500 rpm to prepare the nanocomposite dispersions. Subsequently, the solvent was evaporated by keeping the mixture at room temperature for 12 hours and at 65°C for 8 hours, and the nanocomposite films were obtained. The samples were coded SM40, SM50, and SM60-0, 1, 2, 3, 5 based on their polymer ratios and MWCNT content. The SEM images were captured with a ZEISS Sigma 300 device. SEM analyses were performed in two separate laboratories to verify the reproducibility of the results, and the ZEISS Sigma 300 device was used in both. Similar acceleration voltage and working distance parameters were preferred, resulting in morphological consistency across the obtained images. The XRD peaks were obtained through a PANalytical Empyrean XRD device. The DSC analyses were performed using a Netzsch DSC 3500 Sirius device. The DSC analyses were evaluated based on the initial heating scans to reflect the morphological and kinetic properties of the samples prepared by the solvent-casting method. Interfacial tensions were calculated using the Owens-Wendt approach, which is based on the distribution of surface energy into dispersive and polar components.[17] FTIR peaks were obtained with a Bruker VERTEX 70v device. The TGA/DTG measurements were obtained using the PerkinElmer Diamond TG/DTA system.

3. RESULTS AND DISCUSSION

The localization tendency of nanofillers in phase-separated polymer systems is evaluated within the framework of the wetting coefficient approach, which is widely used in the literature.[18,19] According to this approach, the wetting coefficient criteria is calculated using the component surface energies presented in Table 1.

Table 1. Surface Energies of Nanocomposite Components*

Component	γ (mN/m)	γ^d (mN/m)	γ^p (mN/m)	Ratio used (γ^d/γ^p)	Source
SAN (25% AN)	35.5	28.4	7.1	80/20	[5,13]
PMMA	40.7	28.5	12.2	70/30	[20]
MWCNT-COOH	45.3	24.9	20.4	55/45	[14]

*Polar and dispersive components are given based on the representative ratios reported in the literature.

$$\gamma_{\{12\}} = \gamma_1 + \gamma_2 - 2\left(\sqrt{\{\gamma_1^d \gamma_2^d\}} + \sqrt{\{\gamma_1^p \gamma_2^p\}}\right) \qquad (1)$$

The surface energies presented in Table 1 are substituted into the Owens–Wendt approach (Eq. 1), and the interfacial tensions of the nanocomposite components shown in Table 2 are calculated. The calculated interfacial tensions are then substituted into the equation for wetting coefficient given in Eq. (2) in order to calculate the wetting coefficient (ω_a). Table 2 presents interfacial tensions between components calculated with Eq. (1).

Table 2. Interfacial Tensions Between Components in the SAN/PMMA/MWCNT Nanocomposite*

Interface Pair	Interface Tension (mN/m)	Physical Interpretation
$\gamma_{(MWCNT\text{-}SAN)}$	≈ 6.7	High interfacial tension → Low compatibility
$\gamma_{(MWCNT\text{-}PMMA)}$	≈ 1.9	Low interfacial tension → High compatibility
$\gamma_{(SAN\text{-}PMMA)}$	≈ 1.3	Interphase tension between two polymers

*The surface energy values given in the table are representative singular values reported in the literature and were used to compare the relative interaction tendencies at the polymer–polymer and filler–polymer interfaces of the components rather than solid-gas contact angle-based surface energies.

$$\omega_a = \frac{\left(\gamma_{\frac{PMMA}{MWCNT}} - \gamma_{\frac{SAN}{MWCNT}}\right)}{\gamma_{\frac{SAN}{PMMA}}} \qquad (2)$$

$\gamma_{PMMA/MWCNT}$: Interfacial tension between carbon nanotubes and the PMMA phase (mN/m).

$\gamma_{SAN/MWCNT}$: Interfacial tension between carbon nanotubes and the SAN phase (mN/m).

$\gamma_{SAN/PMMA}$: Interfacial tension between the SAN and PMMA phases (mN/m).

ω_a: Wetting coefficient (unitless)

The wetting coefficient was defined assuming that the MWCNT is located at the SAN-PMMA interface. Here, the numerator term denotes the difference between the interfacial tensions of MWCNT-SAN and MWCNT-PMMA, and the denominator term represents the interfacial tension between the SAN-PMMA phases. When these values between the components were substituted into the wetting coefficient equation (Eq. 2), the value $\omega \approx -3.69$ was obtained. Based on the calculated ω value, the localization tendency of MWCNTs can be interpreted as follows.

Accordingly:

If $\omega > 1$, MWCNTs are thermodynamically located at the SAN phase.

If $-1 < \omega < 1$, MWCNTs are located at the interface of two polymers (at the exact boundary).

If $\omega < -1$, MWCNTs are thermodynamically located at the PMMA phase.

It shows that MWCNTs may exhibit a greater affinity for the PMMA phase, as indicated by the range of values. When the values were substituted into Eq. (2), it was observed that $\omega_a < -1$. This suggests that MWCNTs may show greater affinity to the PMMA phase in particular. Evaluations based on the relevant equations indicate that MWCNT-PMMA interactions may be more convenient than MWCNT-SAN interactions.[21] In this context, it can be said that, under theoretical equilibrium conditions, MWCNTs may preferentially localize in the PMMA phase when the aforementioned equations are used. However, it is known that during the preparation of phase-separated polymer systems, kinetic factors, such as solvent removal kinetics and simultaneous phase solidification, may limit the complete migration of the filler to the phase predicted under equilibrium conditions.[22,23] This may cause MWCNTs to become trapped at the interface between polymer phases rather than showing a distinct phase preference. Therefore, in this study, the wetting coefficient approach provides a theoretical framework suggesting that MWCNTs may exhibit interface localization in the SAN/PMMA system. However, it does not yield a quantitative result. The experimental results supporting this prediction are evaluated below using SEM and XRD analyses.

To identify the hierarchical structure of the mixtures, the contrast differences between the polymer components were enhanced, and the micro-scale phase separation and distribution of phase regions (SAN/PMMA) were investigated. High-resolution shots were used to elaborate the nanoscale distribution of MWCNTs and the localization (wetting) behavior at the interface. Pure samples (−0) and samples with a representative medium MWCNT content (−2) were compared in Figure 1 to clearly show how morphological changes evolved with MWCNT addition.

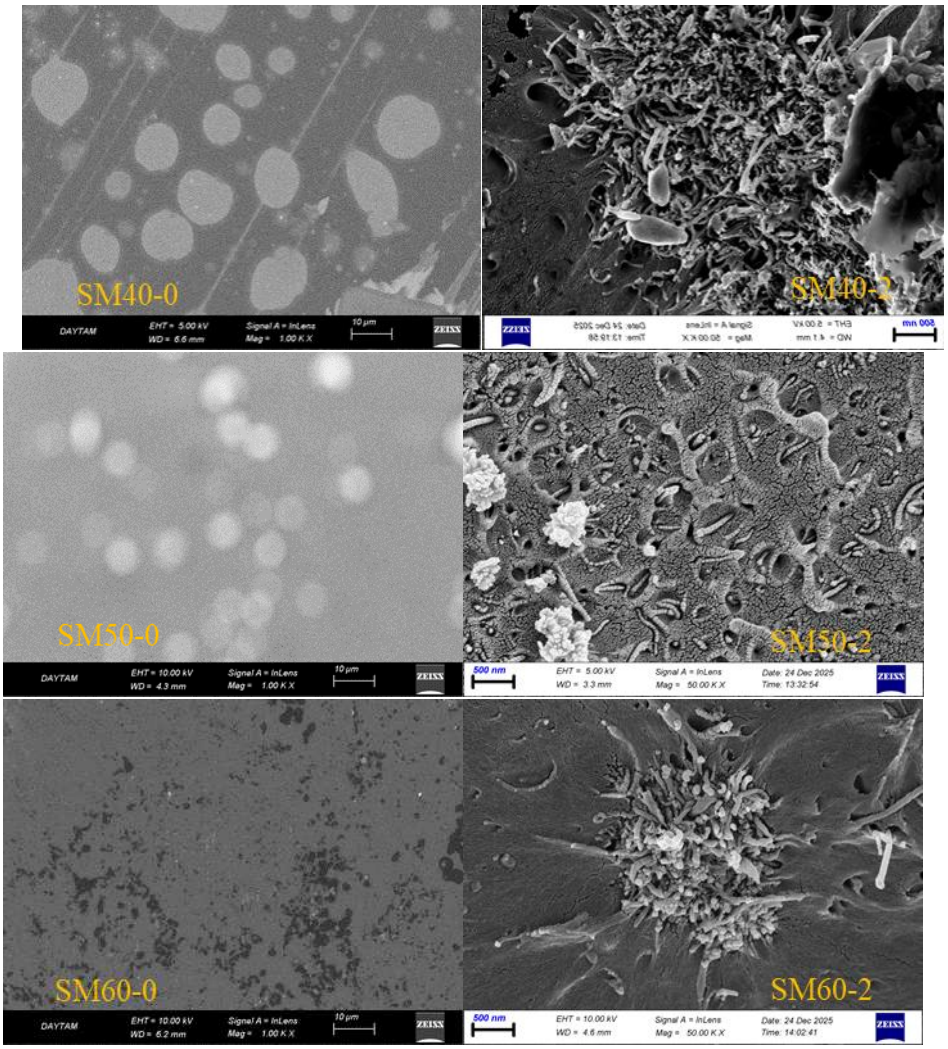


Figure 1. SM40, 50, and 60 (−0 and −2) samples and ZEISS-Sigma 300 images.

SEM images of pure SAN/PMMA blends reveal characteristic morphological structures that vary with composition. While droplet-type phase morphology can be clearly observed in systems with a high PMMA ratio, a transition to a morphological structure is observed, in which droplet boundaries become increasingly uncertain, and both phases attain partial continuity. With the addition of MWCNT, SEM images show that MWCNTs localize mainly along the phase interface, and the interface regions become more identifiable due to their presence. This observation visually supports the tendency of MWCNTs to localize at the interface in the SAN/PMMA system. No extensive micron-scale agglomerates were observed; however, localized MWCNT-rich regions are visible, particularly in the SM60-2 sample. In addition, the short-range ordering detected in the XRD patterns suggests the possible presence of nanoscale MWCNT clusters below the resolution limit of SEM. SEM analyses present detailed information on phase morphology and the selective localization of MWCNTs. In line with the limited miscibility behavior reported in the literature, droplet-type phase separation was

observed in the SAN/PMMA blends.[6,24] Upon adding MWCNT, the droplet structure became significantly thinner, the characteristic phase dimensions were reduced, and the morphology became more homogeneous. This indicates that MWCNTs create a barrier effect, suppressing phase coalescence.

Wetting coefficient (ω) calculations anticipate that MWCNTs thermodynamically tend to be localized at the PMMA phase. In contrast, the SEM analyses revealed that MWCNTs are mainly localized at the SAN/PMMA phase interface. This apparent contradiction can be explained by the fact that the local viscosity, which increases during solvent evaporation, kinetically limits the migration of MWCNTs to the thermodynamically selected phase in systems prepared by the solvent-casting method. MWCNTs fixed at the interface as a result of a dynamic trapping mechanism during this process prevent phase merger, thereby stabilizing morphology. Consequently, the inherent kinetic limitations of solution casting prevented the long-range reorganization of MWCNTs, thereby playing a decisive role in the formation of the observed interface-dominated architecture. The concentration-dependent mobility approach, developed by Cummings et al.[25] to examine changes in solvent evaporation kinetics, shows that system mobility can decrease during solvent evaporation and provides mathematical support for the trapping mechanism. In view of this kinetic limitation mechanism, the trapping of MWCNTs observed in this study at the SAN/PMMA interface can also be explained by kinetic trapping, as viscosity increases and mobility decreases (Eq. 3 and Eq. 4). This kinetic limitation mechanism can be mathematically formulated within a framework in which mobility is concentration-dependent and particle motion is determined by the product of mobility and the energy gradient.

$$\mu_sl = \gamma_sl \cdot \varphi_sl^2 \qquad (3)$$

μ_sl: Mobility (movement capability) of the solvent in the liquid phase
γ_sl: Kinetic coefficient (constant proportionality parameter) of the solvent
φ_sl: Volume fraction of the solvent in the liquid phase.

This equation shows that solvent mobility is proportional to the square of the solvent concentration. As solvent evaporation progresses, φ_sl decreases and, consequently, μ_sl rapidly drops. The second-order decrease in mobility increases system viscosity and kinetically limits diffusion. Therefore, the process of solvent removal does not take place at a constant rate; mobility can be significantly reduced at low solvent ratios, and a certain amount of solvent can be kinetically trapped within the polymer matrix.

$$dx/dt = -\mu \cdot (\delta F/\delta x) \qquad (4)$$

x: Location of the particle (MWCNT)

t: Time

dx/dt: Time-dependent velocity of the particle

μ: Mobility of the particle (ability to move)

F: Total free energy of the system

$\delta F/\delta x$: Derivative of free energy with respect to location (thermodynamic driving force)

This equation states that the velocity of a particle is dependent on the product of its mobility and the thermodynamic driving force. If one phase is preferred in terms of energy (e.g., the PMMA phase), then δF/δx is nonzero, and the system tends towards equilibrium. However, as mobility μ decreases, the movement velocity decreases significantly, even when an energy difference is present. As system viscosity increases during solvent evaporation, reducing mobility, MWCNTs may become kinetically trapped at the interface before reaching the thermodynamically preferred phase.

The observation that MWCNTs are localized at phase interfaces or PMMA-rich regions is consistent with previous studies, which suggest that MWCNT localization is determined by both thermodynamic and kinetic factors.[12,13] MWCNTs that accumulate at the phase interface form a physical barrier that prevents coalescence and contributes to long-term stabilization of the phase morphology. These findings indicate that MWCNTs may play a role not only as a reinforcing filler material but also in regulating morphology. This kinetic trapping mechanism maintains homogeneous chain segment mobility at the macro scale by preventing MWCNTs from embedding in the polymer phases. This is consistent with the observation of a single glass transition temperature (Tg) in all the samples, despite MWCNT addition (Table 3), and can be regarded as an effect that contributes to strengthening the morphological stabilization of the phase rather than impairing MWCNT miscibility. This morphological stabilization not only suppresses phase coalescence but also enables the formation of a MWCNT network geometry sensitive to phase continuity. This is consistent with the increase in activation energy observed in TGA and kinetic analyses; at the same time, it provides the basis of morphology-dependent percolation potential.

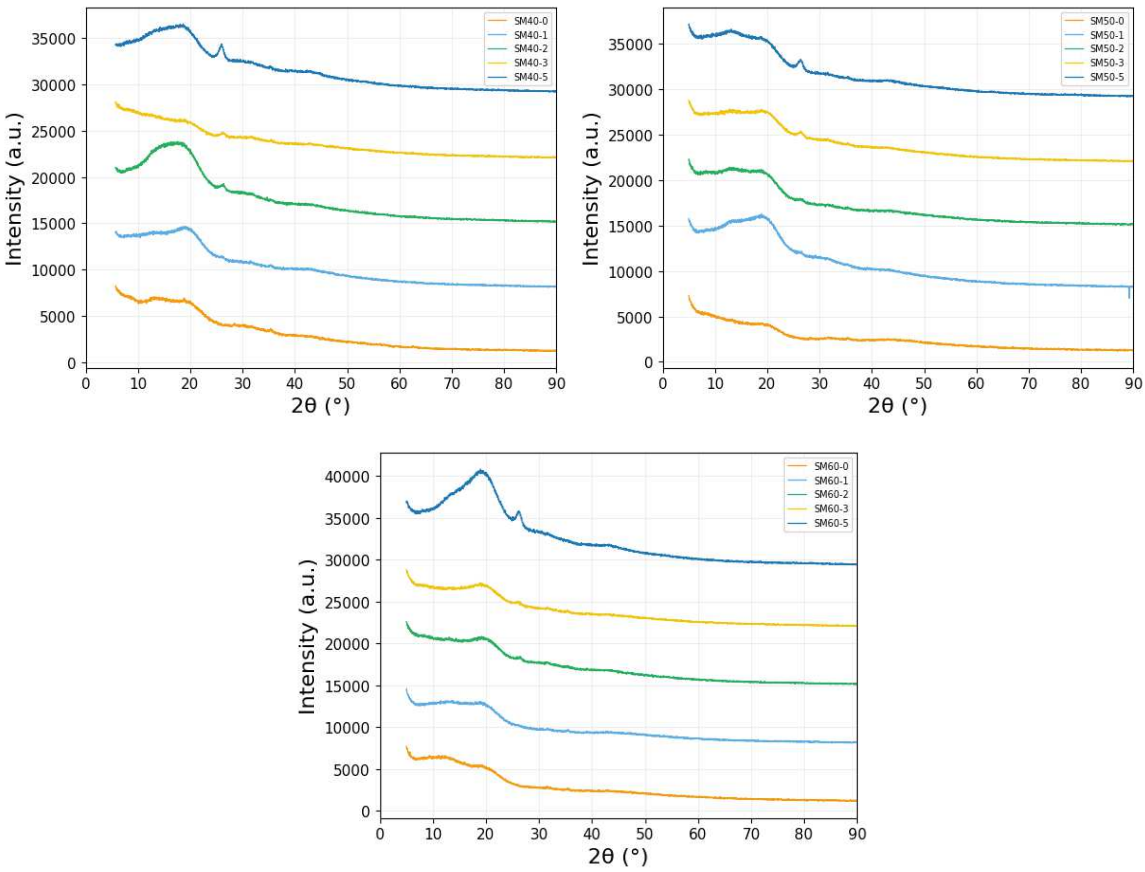


Figure 2. XRD curves of the samples SM40, SM50, SM60 (−0,−1,−2,−3,−5).

XRD analyses revealed that all SAN/PMMA/MWCNT nanocomposites maintain their dominant amorphous character (Figure 2). Broad halos observed within the ranges of 2θ ≈ 18° and 31–32° confirm that polymer matrices do not contain long-range crystalline order. In the XRD data enhanced with the Savitzky-Golay filter, no significant shift was observed in the main amorphous peak positions, notwithstanding the addition of MWCNTs, which indicates that MWCNTs do not alter the average distance between polymer chains at the macro scale.[26]

However, changes in peak intensities and areas under the curve were attributed to local intensity differences arising from selective MWCNT localization rather than crystallization. Weak reflections at 2θ ≈ 26° and 43° suggest that MWCNTs may form local clusters via van der Waals interactions. When evaluated alongside the SEM findings, these results indicate that MWCNTs are not distributed uniformly but are organized into a partially continuous network throughout the system.

Since functionalized MWCNTs were used in this study, FTIR analysis was considered a necessary characterization step to determine whether MWCNT-polymer interactions were of a chemical or secondary physical nature.

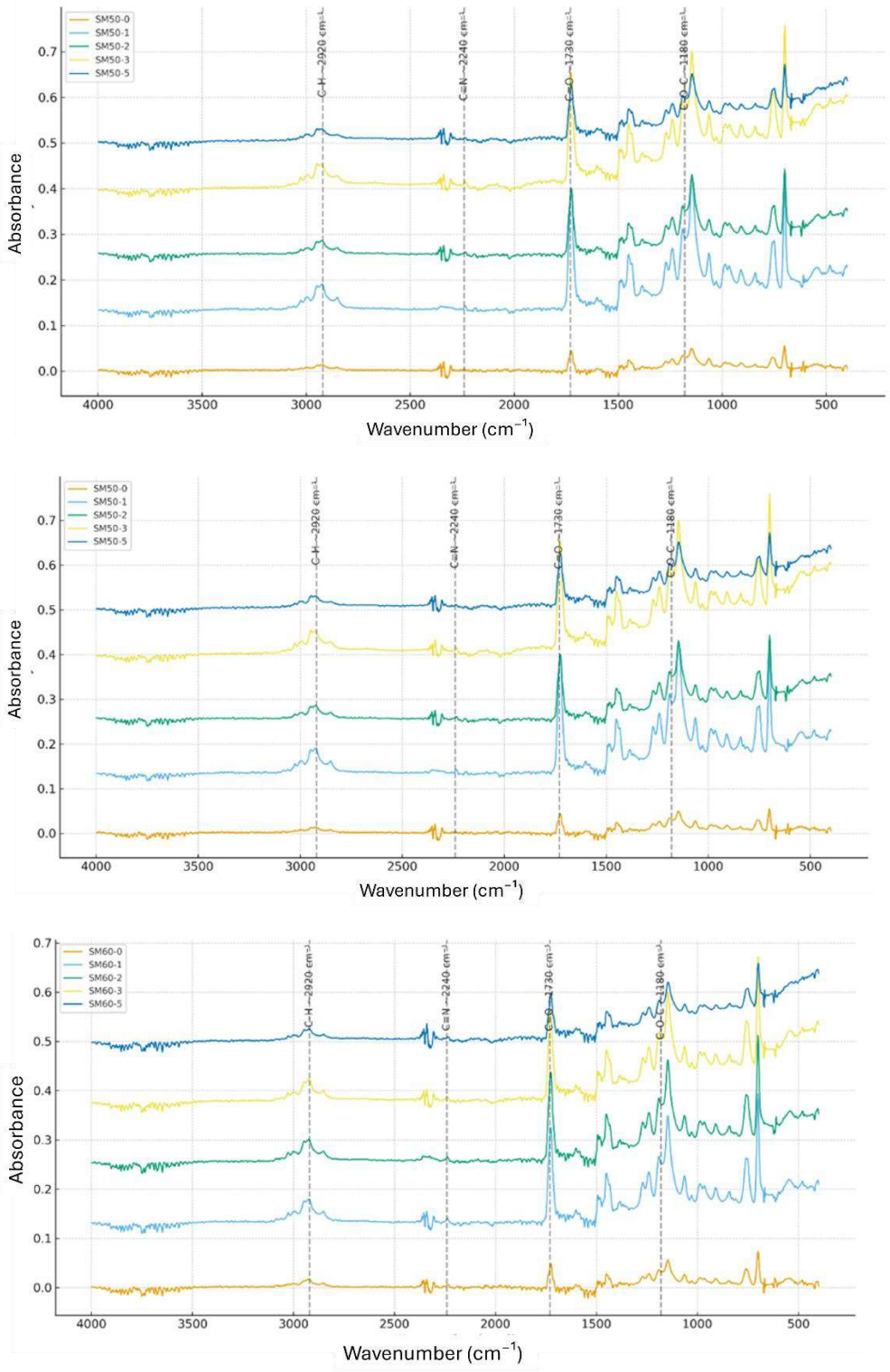


Figure 3. FTIR curves of the samples SM40, SM50, SM60 (−0,−1,−2,−3,−5).

The FTIR spectra (Figure 3) show that the characteristic carbonyl band of PMMA (~1730 cm^{-1}) slightly decreases in intensity upon MWCNT addition while remaining at similar wavenumber positions. No new peak formation or significant wavenumber shift was observed

in the carbonyl region upon MWCNT addition, indicating that no new covalent bonding occurred. The variation in carbonyl band intensity may be associated with changes in the local molecular environment or functional group accessibility induced by the presence of MWCNTs rather than direct chemical bond formation. However, FTIR data alone do not provide definitive evidence for specific electronic interaction mechanisms. When evaluated based on the concept of "functional group accessibility", defined by Coleman et al.[20], the observed decrease in the band intensity can be interpreted as a result of steric shielding and reduced functional-group accessibility caused by the presence of CNTs. On the other hand, the limited changes in the nitrile (~2237 cm^{-1}) and aromatic ring bands of the SAN phase indicate that this effect occurs primarily through the carbonyl groups in PMMA.

Table 3. T_g Values of the Samples SM40, SM50, SM60 (−0,−1,−2,−3,−5)

Sample Code	T_g (°C)	Sample Code	T_g (°C)	Sample Code	T_g (°C)
SM40-0	86.3	SM50-0	85.6	SM60-0	83.6
SM40-1	85.4	SM50-1	83.5	SM60-1	84.5
SM40-2	82.6	SM50-2	82.9	SM60-2	84.7
SM40-3	83.6	SM50-3	86.8	SM60-3	83.2
SM40-5	86	SM50-5	83.5	SM60-5	81.9

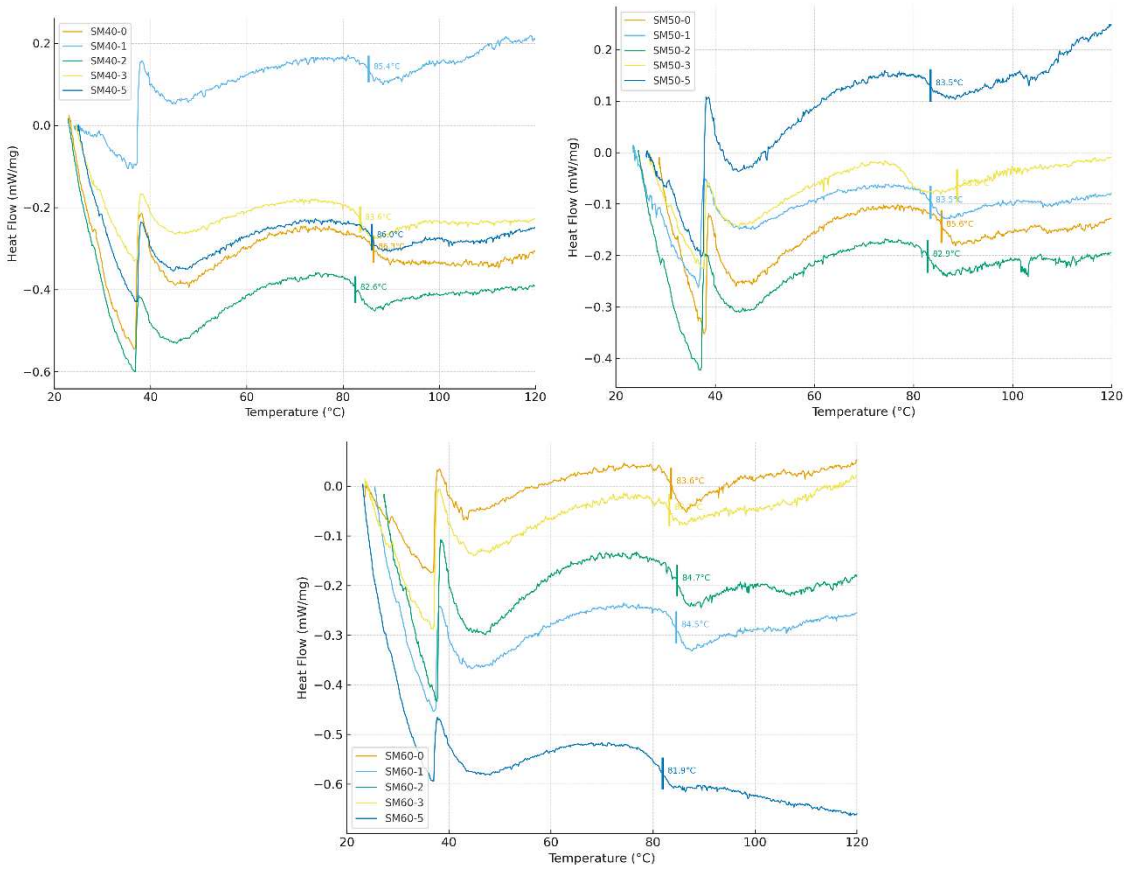


Figure 4. DSC curves of the samples SM40, SM50, SM60 (−0,−1,−2,−3,−5).

The observation of a single glass transition temperature (T_g) in all SAN/PMMA/MWCNT nanocomposites (Table 3 and Figure 4) indicates that the system exhibits homogeneous interphase segmental dynamics on the DSC time scale. Despite MWCNT addition, no significant shift in Tg values or double Tg formation was observed, suggesting that MWCNTs do not suppress polymer chain mobility at the macro scale; instead, they are primarily localized at phase interfaces and provide morphological stabilization. The Tg values reported by Parameswaranpillai et al.[15] correspond to systems prepared by the melt-blending method, whose thermal history has mainly been minimized based on second-heating DSC scans. The present study, however, aims to preserve the kinetic effects of MWCNTs on the phase morphology by using the first heating DSC scans of samples prepared by the solvent-casting method. Within this context, it can be seen that the methodological differences between studies reported in the literature and the present study may be decisive for T_g measurements. According to evaluations of Tg values, SEM, FTIR, and wetting coefficient analyses, the distribution and wetting behavior of MWCNTs mainly affect local-scale chain segment mobility. However, they do not cause a macro-level hardening or plasticizing effect that would disrupt the miscibility character on the DSC time scale. The effect of this microstructural arrangement on mechanical properties can be investigated in greater detail through advanced engineering tests, which quantify parameters such as tensile strength and ductility.

In the literature, polymer–CNT interactions are generally classified into micromechanical interlocking, covalent/ionic bonding, and secondary physical interactions such as van der Waals and electrostatic forces.[12,27] In this study, no bands indicative of new chemical bonds was observed in the FTIR analyses, and MWCNTs were localized at the phase interface in the SEM images, suggesting that MWCNT-polymer integration occurs through secondary physical interactions rather than micromechanical locking or chemical bonding. Furthermore, the increase in viscosity resulting from solvent removal during the casting process kinetically limits the migration of MWCNTs to the thermodynamically preferred phase.

Table 4 and Figure 5 present the results of the TGA analysis. As can be seen at first glance, the contribution of MWCNTs shifts the degradation process and the mass loss of the nanocomposite towards higher temperatures. Moreover, higher amounts of residue (char) were obtained in the MWCNT-added blends compared to the pure blend. Negative char difference values indicate that the residue formed is lower than the theoretical prediction, suggesting that the improvement in thermal stability mainly originates from the barrier effect of MWCNTs rather than synergistic char formation.

Table 4. TGA Results of the Samples SM40, SM50, SM60 (−0,−1,−2,−3,−5)

Sample Code	T1 (°C)	T2 (°C)	T_{max} (°C)	Final % Loss	Residue (%)	Char Difference (%) *
SM40-0	195	390	430	99.3	0.7	-
SM40-1	195	395	445	98.5	1.5	−0.2
SM40-2	200	400	460	97.8	2.2	−0.5
SM40-3	200	405	475	96.8	3.2	−0.5
SM40-5	205	410	490	96.2	3.8	−1.9
SM50-0	190	385	420	98.8	1.2	-
SM50-1	195	390	435	97.5	2.5	0.3
SM50-2	195	395	450	96.8	3.2	0
SM50-3	200	400	470	95.5	4.5	0.3
SM50-5	205	405	485	94.2	5.8	−0.4
SM60-0	185	380	415	97.8	2.2	-
SM60-1	190	385	430	96.4	3.6	0.4
SM60-2	190	390	445	95.6	4.4	0.2
SM60-3	195	395	465	94.8	5.2	0
SM60-5	200	400	480	93.5	6.5	−0.7

Char difference (%) * refers to synergistic residue increase that is calculated considering the content of pure blend and MWCNT.

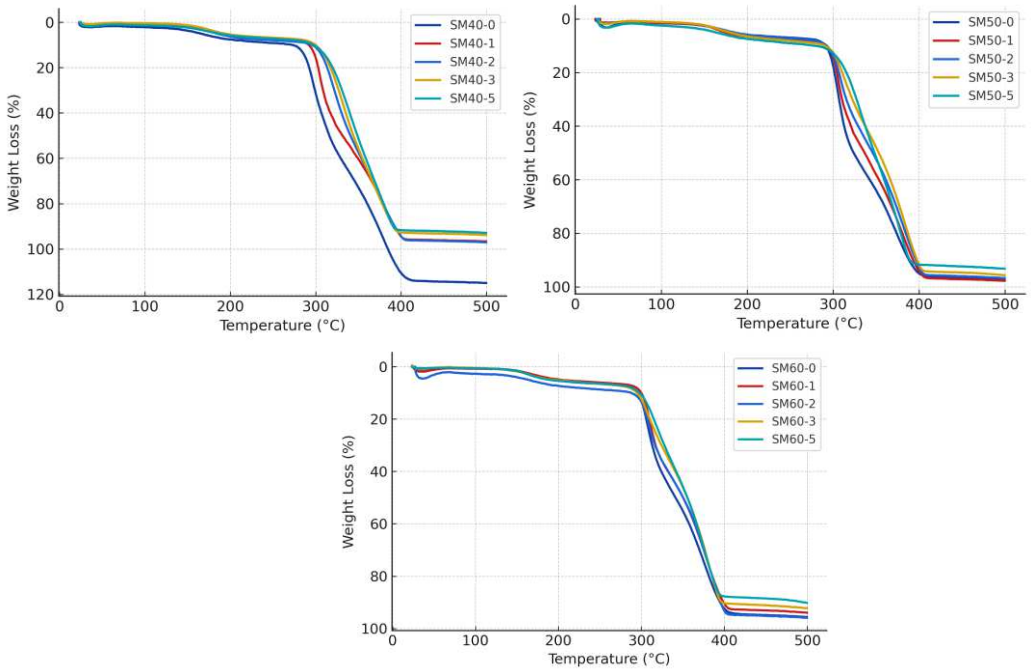


Figure 5. TGA curves of the samples SM40, SM50, SM60 (−0,−1,−2,−3,−5).

The structures of MWCNTs with high specific surface areas allow polymer chains to adsorb onto their surfaces. It is thought that a carbon-rich carbonaceous char layer forms around the MWCNTs when the polymer segments attached to this surface degrade during heating. This layer physically slows down heat transfer to the polymer regions covered by the MWCNT network, thus helping protect the underlying matrix at higher temperatures. Therefore, degradation processes occurring outside the MWCNT network are also indirectly delayed. This

is manifested in degradation temperatures shifting to higher values in the TGA curves and the formation of more residue (char) at the end of degradation. These observations are consistent with the barrier effect reported in MWCNT-containing nanocomposites. This physical protective effect is consistent with the mechanism often described in the literature as the "barrier effect" or "labyrinth effect" in CNT-reinforced systems.[28,29] The differences in char values presented in Table 4 reveal a systematic increase in the amount of residue with the addition of MWCNT, consistent with thermal degradation shifting to higher temperatures. The SM50 series (SAN50/PMMA50) showed the most balanced thermal response in the study. The main reason for this balanced response may be that the MWCNT localization behavior predicted by wetting coefficient (ωa) calculations and the phase morphology formed in this series exhibit a coherent structure. The balanced distribution of SAN and PMMA phases enabled MWCNTs to form a MWCNT arrangement with local connections within the matrix, thereby allowing the formation of the most effective protective char-shielding. Thanks to this morphological advantage, the SM50 group displayed the highest thermal stability, as evidenced by the distinctive increase in T_{max} values and the positive char difference.

Compared to the SM40 series, which has a higher PMMA content, the SM50 group exhibits higher performance, which is directly related to the morphological arrangement of the polymer phases. The probable co-continuous structure observed at a 50/50 composition ratio enabled MWCNTs to form a more effective network within PMMA-rich channels; thus, MWCNTs created a denser barrier effect in the matrix, and both T_{max} values increased, and carbonization synergy became more efficient compared to the SM40 series.

These observations are directly associated with the increases in thermal stability observed in the TGA and DTG analyses. The network structure formed by MWCNTs in the matrix creates a tortuous path mechanism that impedes the diffusion of volatile degradation products generated during thermal degradation, thereby delaying the degradation process.[28,29] In parallel, weak reflections around $2\theta \approx 26°$ in the XRD analyses suggest that MWCNTs may exhibit a tendency towards microscale agglomeration in certain regions, consistent with SEM observations.

Figure 6 and Table 5 present the DTG curves showing the mass-loss/degradation rates in thermal analyses, along with the results of Coats and Redfern[30] calculations based on these data.

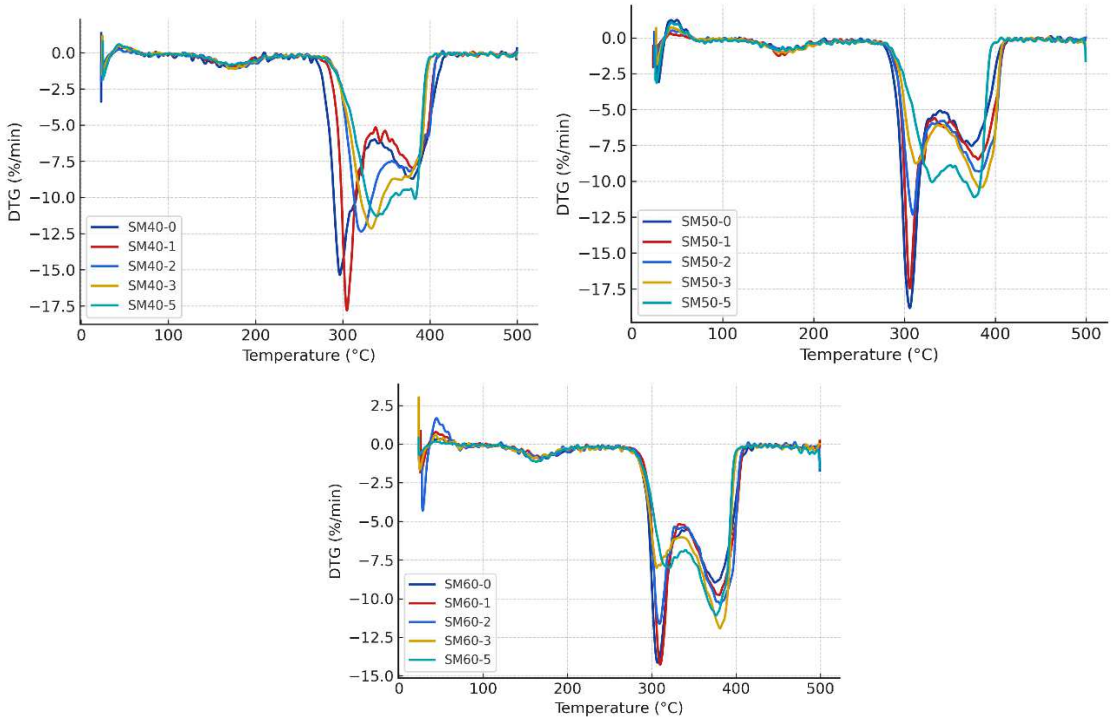


Figure 6. DTG curves of the samples SM40, SM50, SM60 (−0,−1,−2,−3,−5).

Table 5. Ea (activation energy) Data of the Samples SM40, SM50, SM60 (−0,−1,−2,−3,−5)

Sample Code	MWCNT Content (w %)	Ea (kJ/mol)	Correlation Coefficient (R^2)	ΔEa (kJ/mol)*
SM40-0	0	142.5	0.996	-
SM40-1	1	151.8	0.994	+9.3
SM40-2	2	164.2	0.997	+21.7
SM40-3	3	178.4	0.995	+35.9
SM40-5	5	185.6	0.992	+43.1
SM50-0	0	138.4	0.995	-
SM50-1	1	146.2	0.993	+7.8
SM50-2	2	158.7	0.996	+20.3
SM50-3	3	169.4	0.994	+31.0
SM50-5	5	176.1	0.992	+37.7
SM60-0	0	129.2	0.997	-
SM60-1	1	139.5	0.995	+10.3
SM60-2	2	152.8	0.998	+23.6
SM60-3	3	165.3	0.996	+36.1
SM60-5	5	174.8	0.994	+45.6

* The ΔEa value represents the increase in activation energy based on the relevant pure polymer matrix.

The TGA and DTG analyses revealed that the addition of MWCNT systematically increased thermal stability across all SAN/PMMA series. The increase in degradation temperatures (T_2 and T_{max}) with rising MWCNT content confirms that MWCNTs create a physical barrier effect within the polymer matrix. The low mass losses observed at approximately 200°C were attributed to the removal of moisture and volatile solvent residues in the structure and do not

have a direct relation with main-chain degradation.[31] The char difference (ΔW) was calculated in Eq. (5) as the difference between the experimentally measured residue of the composite and the theoretical residue estimated from the weighted contributions of its individual components:

$$\Delta W = \frac{W_{\exp} - (m_p W_p + m_{MWCNT} W_{MWCNT})}{m_p + m_{MWCNT}} \qquad (5)$$

where W_{exp} is the experimental residual mass (%) of the composite obtained from thermogravimetric analysis (TGA), W_p is the residual mass (%) of the neat polymer blend (without MWCNT), and W_{MWCNT} is the residual mass (%) of pure MWCNT under identical TGA conditions. MWCNT content was defined as 1, 2, 3, and 5 wt% relative to the fixed polymer blend mass rather than the total composite mass. The parameters m_p and m_{MWCNT} represent the masses of the polymer blend and MWCNT used in the composite formulation, respectively. In the present study, the polymer blend mass (m_p) was kept constant for all formulations. MWCNT content was defined as 1, 2, 3, and 5 wt% relative to this fixed polymer mass rather than the total composite mass. Accordingly, the amount of MWCNT incorporated into each formulation corresponded to the selected weight percentage of the polymer blend mass. In other words, the MWCNT mass was determined as the chosen wt% of the constant polymer mass used in the formulation. MWCNT loadings were defined relative to the constant polymer matrix mass rather than the total composite mass in order to enable a controlled and systematic evaluation of the effects of varying MWCNT contents while maintaining a fixed polymer matrix throughout the experiments. Since MWCNT was introduced relative to a fixed polymer mass, the total composite mass increased with increasing MWCNT loading. Therefore, the theoretical residue was calculated by normalizing the weighted residue contributions of the polymer blend and MWCNT to the total mass of the composite ($m_p + m_{MWCNT}$), ensuring a consistent and physically meaningful comparison among all formulations.

Peak broadening and a decrease in intensity observed in the DTG curves indicate that MWCNT addition limits the mobility of polymer chains and slows down degradation kinetics. The systematic increase in activation energies (E_a) calculated through the Coats–Redfern Equation can be regarded as a quantitative indicator of this kinetic limitation (Eq. 6). The reason why this method was preferred is that it is suitable for analyses that occur at a single heating rate; however, it should be stressed that the approach used in the study aims to comparatively reveal the change in the relative energy barrier that must be overcome for degradation with MWCNT addition rather than defining the degradation mechanism in detail. In this regard, in line with the widely recognized assumption in the literature regarding polymer degradation, the reaction order was set to n = 1.

$$\ln\left(\frac{(-\ln(1-\alpha))}{T^2}\right) = \ln\left(\frac{(A\,R)}{(\beta\,E)}\right) - \frac{E}{(R\,T)} \qquad (6)$$

This analysis was used to quantitatively compare the change in the relative energy barrier resulting from the addition of MWCNT to the thermal degradation process in SAN/PMMA nanocomposite systems. In particular, the increase in the E_a value in the SM60 series by approximately 45 kJ/mol with the addition of 5% MWCNTs clearly demonstrates that MWCNTs raise the energy barrier that must be overcome for degradation. The high correlation coefficients obtained in the study ($R^2 > 0.99$) show that the preferred kinetic model is consistent with experimental data.[29]

4. CONCLUSIONS

This study systematically investigated the influence of multi-walled carbon nanotube (MWCNT) addition on the morphology and thermal behavior of SAN/PMMA blend systems, with particular emphasis on MWCNT localization. SEM analyses revealed that MWCNTs preferentially localize at the SAN/PMMA phase interface, refining droplet-type morphology and suppressing phase coalescence through a physical barrier effect. Wetting coefficient calculations predicted thermodynamic preference toward the PMMA phase; however, solvent evaporation-induced kinetic limitations restricted MWCNT migration, leading to interface trapping and the formation of an interface-dominated architecture.

FTIR and XRD analyses confirmed that MWCNT incorporation did not induce new chemical bonding or crystallinity but instead modified the microstructural organization through secondary physical interactions and selective localization. The observation of a single T_g across all compositions indicates that this interfacial stabilization does not disrupt segmental homogeneity on the DSC time scale. Thermogravimetric analyses demonstrated a systematic increase in degradation temperatures, residue formation, and activation energy with increasing MWCNT content. The Coats–Redfern kinetic evaluation quantitatively showed that the activation energy increased by up to ~45 kJ/mol at 5 wt% MWCNT loading, confirming that the discontinuous MWCNT network at the phase interface imposes an additional energy barrier to thermal degradation through a barrier/labyrinth mechanism.

Overall, the results demonstrate that MWCNTs function not only as reinforcing nanofillers but also as morphological regulators that govern phase stability and degradation kinetics through selective interfacial localization. The morphology-dependent MWCNT network architecture established in this study provides a structural basis for potential functional

enhancements in thermal and electrical transport, which will be quantitatively addressed in future work.

ASSOCIATED CONTENT

Data Availability Statement

Data will be made available on request.

AUTHOR INFORMATION

Corresponding Author

Afsar Celik − Institute of Natural and Applied Sciences, Van Yuzuncu Yil University, Van, Turkey; https://orcid.org/0000-0002-5824-8338

Author

Gulsen Tozsin − Department of Metallurgical and Materials Engineering, Ataturk University, Erzurum, Turkey; https://orcid.org/0000-0001-5653-9919;

E-mail: gulsentozsin@gmail.com

Declaration of competing interest

The authors declare no conflict of interest.

Authors Contributions

Afsar Celik: Writing –original draft, Methodology, Investigation, Formal analysis, Data curation, Conceptualization. Gulsen Tozsin: Writing –review & editing, Visualization, Validation, Supervision, Resources, Project administration, Methodology, Investigation, Data curation, Conceptualization.

ACKNOWLEDGMENT

This study was supported by the Scientific Research Projects Coordination Unit of Atatürk University (BAP) under Project No. FCD-2025-15155.0.

AI Usage Declaration:

Artificial Intelligence (AI) Usage and Ethical Compliance Statement

The authors hereby declare that no generative artificial intelligence (AI) tools were used to produce, interpret, manipulate, or generate any scientific data, experimental results, numerical analysis, or conceptual conclusions presented in this manuscript.

All experimental procedures, observations, data analyses, scientific interpretations, and theoretical evaluations were entirely conducted and validated by the authors in accordance with accepted academic and research integrity standards.

A large-language-model assistant (ChatGPT) was employed solely for auxiliary

purposes, including:

 Linguistic refinement,

 Clarity enhancement,

 Structural editing of paragraphs,

 Technical formatting of references, and

 Correction of citation order and document coherence.

No part of the scientific content, research design, hypotheses, or conclusions was generated by AI.

The authors retained full intellectual control and responsibility over the manuscript at every stage.

This declaration is made in accordance with the ethical guidelines of:

 COPE (Committee on Publication Ethics),

 Elsevier AI Policy (2023),

 Wiley Author Guidelines for AI Tools (2023),

 Springer Nature AI Disclosure Standards (2023), and

 institutional research integrity frameworks.

The authors acknowledge that they are solely accountable for the accuracy, validity, and originality of the manuscript's scientific content.

REFERENCES

(1) L.A. Utracki, Commercial polymer blends, Chapman and Hall, London (1998).

(2) Plastics Europe, Plastics–the fast facts 2023. https://plasticseurope.org/knowledge-hub/plastics-the-fast-facts-2023/ Accessed: 01/07/2025.

(3) I.C. Sanchez, Polymer compatibility and incompatibility: principles and practices. K. Solc (Ed.), MMI Press, Harwood (1982).

(4) T.A. Osswald, G. Menges, Materials science of polymers for engineers, third edition, Hanser (2012).

(5) J.E. Mark, Polymer data handbook, Oxford University Press (1999).

(6) J. Resch, J. Dreier, C. Bonten, M. Kreutzbruck, Miscibility and phase separation in PMMA/SAN blends investigated by nanoscale AFM-IR, Polymers 13 (21) (2021) 3809, https://doi.org/10.3390/polym13213809.

(7) J.K. Pandey, K.R. Reddy, A.K. Mohanty, M. Misra, Handbook of polymer nanocomposites: processing, performance and application–Volume A: Layered

Silicates. Springer-Verlag Berlin Heidelberg (2014), https://doi.org/10.1007/978-3-642-38649-7.

(8) A.O. Adeola, P.N. Nomngongo, Advanced polymeric nanocomposites for water treatment applications: a holistic perspective, Polymers 14 (12) (2022) 2462, https://doi.org/10.3390/polym14122462.

(9) W. Bauhofer, J.Z. Kovacs, A review and analysis of electrical percolation in carbon nanotube polymer composites, Compos. Sci. Technol. 69 (10) (2009) 1486–1498, https://doi.org/10.1016/j.compscitech.2008.06.018.

(10) Y. Zhou, R. Azumi, Carbon nanotube based transparent conductive films: progress, challenges, and perspectives, Sci. Technol. Adv. Mater. 17 (1) (2016) 493-516, https://doi.org/10.1080/14686996.2016.1214526.

(11) H. Li, Y. Qian, X. Zhou, Z. Zhang, Functionalization of carbon nanotubes in polystyrene and styrene–acrylonitrile composite systems, Polymers 16 (6) (2024) 770, https://doi.org/10.3390/polym16060770.

(12) X.D. Qi, J.H. Yang, N. Zhang, T. Huang, Z.W. Zhou, I. Kühnert, P. Pötschke, Y. Wang, Selective localization of carbon nanotubes and its effect on the structure and properties of polymer blends, Prog. Polym. Sci. 123 (2021) 101471, https://doi.org/10.1016/j.progpolymsci.2021.101471.

(13) S.H. Yang, J.W. Lee, H. Kim, Localization behavior of multi-walled carbon nanotubes in ternary blends of PC, SAN, and PMMA, Korea Aust. Rheol. J. 32 (2) (2020) 145–152, https://doi.org/10.1007/s13367-020-0013-6.

(14) V. Mittal, Characterization techniques for polymer nanocomposites, Wiley-VCH Verlag GmbH & Co KGaA (2012), https://doi.org/10.1002/9783527654505.

(15) J. Parameswaranpillai, G. Joseph, S.K. Sidhardhan, S. Jose, N. Hameed, Miscibility, UV resistance, thermal degradation, and mechanical properties of PMMA/SAN blends and their composites with MWCNTs, J. Appl. Polym. Sci. 133 (30) (2016), https://doi.org/10.1002/app.43628.

(16) A. Celik, Preparation and characterization of carbon nanotube doped PMMA/PVC nanocomposite (Doctoral dissertation), Van Yuzuncu Yil University, Graduate School of Natural and Applied Sciences, Van, Türkiye (2022).

(17) D.K. Owens, R.C. Wendt, Estimation of the surface free energy of polymers, J. Appl. Polym. Sci. 13 (8) (1969) 1741–1747, https://doi.org/10.1002/app.1969.070130815.

(18) S. Wu, Calculation of interfacial tension in polymer systems, J Polym. Sci. Part C: Polymer Symposia 34(1) (1971) 19–30, https://doi.org/10.1002/polc.5070340105.

(19) M. Sumita, K. Sakata, S. Asai, K. Miyasaka, H. Nakagawa, Dispersion of fillers and the electrical conductivity of polymer blends filled with carbon black, Polym. Bull. 25 (2) (1991) 265–271, https://doi.org/10.1007/BF00310802.

(20) M.M. Coleman, G.J. Pehlert, P.C. Painter, Functional group accessibility in hydrogen bonded polymer blends, Macromolecules 29 (21) (1996) 6820–6831, https://doi.org/10.1021/ma9604045.

(21) A. Göldel, A. Marmur, G.R. Kasaliwal, P. Pötschke, G. Heinrich, Shape-dependent localization of carbon nanotubes and carbon black in an immiscible polymer blend during melt mixing, Macromolecules 44 (15) (2011) 6094–6102, https://doi.org/10.1021/ma200793a.

(22) P. Pötschke, T.D. Fornes, D.R. Paul, Rheological behavior of multi-walled carbon nanotube/polycarbonate composites, Polymer 43 (11) (2002) 3247–3255, https://doi.org/10.1016/S0032-3861(02)00151-9.

(23) P. Pötschke, S. Pegel, M. Claes, D. Bonduel, A novel strategy to incorporate carbon nanotubes into thermoplastic matrices, Macromol. Rapid Commun. 29 (3) (2008) 244–251, https://doi.org/10.1002/marc.200700637.

(24) E. Chehrazi, N. Taheri-Qazvini, Segmental dynamics and cooperativity length of PMMA/SAN miscible blend intercalated in organically modified nanoclay, Langmuir 34 (47) (2018) 14358–14367, https://doi.org/10.1021/acs.langmuir.8b03160.

(25) J. Cummings, J.S. Lowengrub, B.G. Sumpter, S.M. Wise, R. Kumar, Modeling solvent evaporation during thin film formation in phase separating polymer mixtures. Soft Matter 2018;14(10):1833–1846. https://doi.org/10.1039/c7sm02560b.

(26) A. Savitzky, M.J. Golay, Smoothing and differentiation of data by simplified least squares procedures, Anal. Chem. 36 (8) (1964) 1627–1639, https://doi.org/10.1021/ac60214a047.

(27) J. Chen, J. Yang, W. Song, D. Xu, Interfacial characteristics of carbon nanotube–polymer composites: a review, Compos A: Appl. Sci. Manuf. 114 (2018) 149–169. https://doi.org/10.1016/j.compositesa.2018.08.021.

(28) T. Kashiwagi, F. Du, K.I. Winey, K.M. Groth, J.R. Shields, S.P. Bellayer, H. Kim, J.F. Douglas, Flammability properties of polymer nanocomposites with single-walled carbon nanotubes: effects of nanotube dispersion and concentration, Polymer 46 (2) (2005) 471–481, https://doi.org/10.1016/j.polymer.2004.10.087.

(29) C. Di Blasi, A. Galgano, C. Branca, Modeling the thermal degradation of poly (methyl methacrylate)/carbon nanotube nanocomposites, Polym. Degrad. Stab. 98 (1) (2013) 266–275, https://doi.org/10.1016/j.polymdegradstab.2012.10.001.

(30) A.W. Coats, J.P. Redfern, Kinetic parameters from thermogravimetric data, Nature 201 (1964) 68–69, https://doi.org/10.1038/201068a0.

(31) L.A.F. Coelho, S.H. Pezzin, M.R. Loos, L.A.S.A. Prado, A.M. Ramirez, Polymer matrix nanocomposites and nanostructured materials, J. Nanomater. 1 (2012) 962815, https://doi.org/10.1155/2012/962815.